

# Is The Leader Robot an Adequate Sensor for Posture Estimation and Ergonomic Assessment of A Human Teleoperator?

Amir Yazdani<sup>\*</sup>, Roya Sabbagh Novin<sup>\*</sup>, Andrew Merryweather<sup>\*</sup>, and Tucker Hermans<sup>†</sup>

**Abstract**—Ergonomic assessment of human posture plays a vital role in understanding work-related safety and health. Current posture estimation approaches face occlusion challenges in teleoperation and physical human-robot interaction. We investigate if the leader robot is an adequate sensor for posture estimation in teleoperation and we introduce a new probabilistic approach which relies solely on the trajectory of the leader robot for generating observations. We model the human using a redundant, partially-observable dynamical system and we infer the posture using a standard particle filter. We compare our approach with posture from a commercial motion capture system and also two least-squares optimization approaches for human inverse kinematics. The results reveal that the proposed approach successfully estimates human postures and ergonomic risk scores comparable to those estimates from gold-standard motion capture. The supplementary materials are available at <https://sites.google.com/view/posture-estimation-in-teleop>

## I. INTRODUCTION

Posture<sup>1</sup> estimation refers to the process of estimating the kinematic or skeletal configuration of the human body including segment lengths and joint angles. In addition to human biomechanics research, human posture estimation is an important part of perception when humans interact with robots and other smart agents (i.e. collaborative robots [1], companion mobile robots [2] and self driving cars [3]). In comparison to deterministic approaches, probabilistic estimation of posture provides more information to plan safer interactions in motion planning around humans [4], hand-over applications [5], and physical interaction in shared-control applications (e.g. teleoperation) [6].

Work-related musculoskeletal disorders (WMSDs) are the 2<sup>nd</sup> largest cause of disabilities worldwide [7] and awkward postures are known to contribute to WMSDs. Teleoperation is a well suited alternative for high-risk tasks (e.g. construction and handling hazardous materials), since the the remote workstation for teleoperator can be designed ergonomically [8]. In this paper, we focus on the problem of posture estimation to assess the ergonomics and risk of WMSDs in teleoperation tasks. Specifically, we investigate if the trajectory information of the leader robot provides adequate sensory information for probabilistic posture estimation for ergonomics assessment.

Collecting accurate and continuous posture data to determine a risk score over a work shift or entire task cycle can be

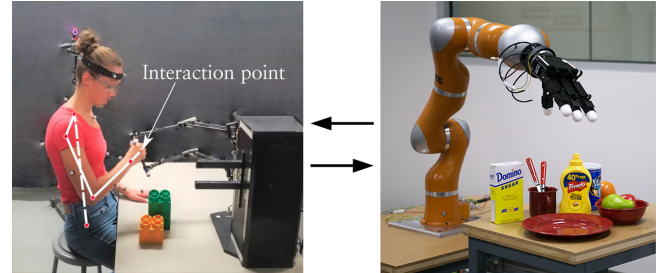


**Fig. 1:** Teleoperation setup for human subject experiments including a Quanser HD<sup>2</sup> haptic interface. Reflective markers on the subject's body are only used for comparison with a MoCap system.

tedious. Early efforts to improve the efficiency of ergonomic assessments include using motion capture (MoCap) systems to estimate the posture and task parameters (e.g. frequency and duration of the task). Although these approaches are fast and accurate, they require significant time and effort for set up [9]. Moreover, putting markers on human operators can be inconvenient. Alternative markerless techniques are more adaptable, minimally intrusive, and less expensive. However, they need calibration to deal with errors and uncertainties from the sensors [10], [11]. The most minimally-invasive, vision-based markerless methods rely on external RGB or RGB-D cameras. These approaches are easily perturbed by the magnitude of the light, background color and even the user's clothing [12]. In teleoperation, a human teleoperator uses a leader robot to move a follower robot during a task. Using the leader robot in such close proximity to the human teleoperator increases occlusion and makes it even more difficult to accurately estimate posture using both markerless and marker-based applications as mentioned in [13].

In this paper, we propose an alternative non-invasive and probabilistic approach that estimates the posture without using any additional sensors beyond the leader robot necessary for the teleoperation. The proposed approach could be used either stand-alone for monitoring the teleoperator posture or in combination with other approaches in a multi-modal sensory system to provide robust posture estimation when occlusion occurs. Although accurate posture estimation for a highly-redundant 10-DOF human model including torso and arm is challenging using only minimum sensory information from the leader robot, we believe that our approach is accurate enough for the application of continuous monitoring of the posture to inform further ergonomic assessments.

We formalize posture estimation as a probabilistic inference problem, in which we measure the leader robot's trajectory (pose and velocity) as the observation and infer the unobserved human posture (joint angles and angular

<sup>\*</sup>Department of Mechanical. Eng. and Robotics Center, University of Utah, Salt Lake City, UT, USA, [amir.yazdani@utah.edu](mailto:amir.yazdani@utah.edu)

<sup>†</sup>School of Computing and Robotics Center, University of Utah, Salt Lake City, UT, USA

<sup>1</sup>Different communities use different terms. We use 'posture' because 'pose' estimation could be misconstrued as a 6-DOF pose of a rigid body.

velocities). We encode human factors and biomechanics knowledge into our partially observable dynamic model. We use the *circle point analysis* (CPA) [14] for segment length estimation of the human body and compare it with anthropometry models. We also impose physical limits on joint angles and check the feasibility of the posture based on the pose-dependant ranges of human motion provided by [15]. We incorporate multiple observations over time enabling us to perform inference using a standard particle filter. We use the estimated posture over the course of the task to assess the user's risk of WMSDs using RULA [16], a standard measure in the ergonomics and safety community. We conduct a human subject study to evaluate our method across 8 users. Moreover, we compare the posture estimation results from the particle filter with the results from well-known deterministic solvers for least-squares optimization. Fig. 1 shows the teleoperator workstation setup we examined. Below, we summarize our main contributions:

1. We formulate the problem of human posture estimation as a partially observable dynamical system that uses only the leader robot's stylus trajectory as the observation.
2. We solve the partially observable problem of human posture estimation from the robot trajectory using a particle filter considering posture feasibility, and compare the results with other deterministic least square solvers.
3. We provide a systematic RULA analysis and compare RULA scores from our estimated posture and the posture estimated with a MoCap system.
4. We compare three different methods for human body segment length estimation: (1) manual measurement of segment length on subjects; (2) measuring the subject height and using an ANSUR II model to calculate the length of the rest of segments; and (3) circle point analysis (CPA) using collected data for each subject during calibration motion routines.

## II. RELATED WORK

In physical human-robot interaction and teleoperation, different methods have been used by researchers to estimate a user's posture, especially for hand gestures [17]–[19]. In all of these approaches, a vision system or IMU sensors were the key additional sensors used for posture estimation. The idea of solely using the leader robot's trajectory for posture estimation of teleoperators has been introduced concurrently with this research by Rahal et al. in [6], where they solved the IK of the 7-DOF human arm. Unlike our probabilistic approach, which can encode a distribution of arm postures, they rely on heuristics to resolve the redundant IK. In addition to their deterministic estimated posture, the heuristic for redundancy resolution does not always hold across different tasks (e.g. some tasks might require the teleoperator to use a working mode different from the working mode of the neutral posture) where the approach in [6] will fail.

The application of particle filters in human posture estimation is extensively discussed in the literature [20]–[22]. The sampling base of particle filters makes them well suited to human posture estimation due to their ability to handle the nonlinearities of human motion [23]. Moreover, the

output estimation is a probabilistic distribution that preserve different working modes of human posture. However, the high dimension of human motion requires a high number of particles to achieve accurate estimation.

Defining a model for human joint limits is challenging. Studies show that the range of motion (ROM) for a joint varies depending on the positions of other joints (inter-joint dependency) or other degrees-of-freedom in the same joint (intra-joint dependency) [15], [24] and vary by gender and person. Akhter et al. [25] used a dataset of recorded MoCap of human motion to develop a discontinuous mathematical model for pose-dependant ROM and check the validity of a full-body posture. Jiang et al. [15] used the above model to label the validity of a set of randomly-generated postures and learned a differentiable neural network based on the generated data and used it as a constraint in the inverse kinematics optimization. Their arm model only includes shoulder and elbow and not the wrist. We use this learned network for checking the validity of the arm posture.

Studies show that evaluating ergonomics to improve working postures reduces the number of WMSDs [26], [27]. Among all the risk assessment tools, RULA [16] and REBA [28] rely mostly on the human posture (i.e. joint angles) and target the human upper body and whole body, respectively. This makes the RULA more suitable for analyzing upper extremity tasks that are common during teleoperation.

## III. PROBLEM STATEMENT

We seek to solve the problem of estimating the human joint-space trajectory in teleoperation using only the observed task-space poses and velocities of the leader robot. We model the physical interaction between the human and the leader robot as an interaction point where the human kinematic chain makes contact with the robot's stylus (Fig. 1).

The state variables of the human include posture (joint angles)  $\mathbf{q}$  and angular velocities  $\dot{\mathbf{q}}$ . They map into the state variables of the stylus through the kinematics of the human model parameterized by the segment length  $\psi$ . We estimate  $\psi$  independently, prior to posture estimation. At each time step, the robot provides an observation as a task-space pose  $\mathbf{z}$  and velocity  $\dot{\mathbf{z}}$  of the stylus at the interaction point,

$$[\mathbf{z}_t; \dot{\mathbf{z}}_t] = h(\phi([\mathbf{q}_t; \dot{\mathbf{q}}_t], \psi)) \quad (1)$$

where  $h$  is the observation function and  $\phi$  is the forward kinematics of the human model. This defines only a partial observation of the human posture, because of redundancy in the human kinematics and a noisy measurement at the interaction point, which may change slightly during a task.

We seek to estimate  $\tau = [[\mathbf{q}_t; \dot{\mathbf{q}}_t], t = 1, \dots, T]$  given the stylus trajectory  $\mathcal{Z} = [[\mathbf{z}_t; \dot{\mathbf{z}}_t], t = 1, \dots, T]$  that predicts a stylus pose closest to the observed stylus pose and obeys the human motion model  $f$  (Eqs. 3 and 4):

$$\begin{aligned} \tau^* = \arg \min_{\tau} & \sum_{t=1}^T ||\phi([\mathbf{q}_t; \dot{\mathbf{q}}_t], \psi) - [\mathbf{z}_t; \dot{\mathbf{z}}_t]||^2 + \\ & ||[\mathbf{q}_t; \dot{\mathbf{q}}_t] - f(\mathbf{q}_{t-1}, \dot{\mathbf{q}}_{t-1}, \psi)||^2 \quad (2) \\ \text{s.t.} & \quad \mathbf{q}_{\min} \leq \mathbf{q} \leq \mathbf{q}_{\max} \end{aligned}$$

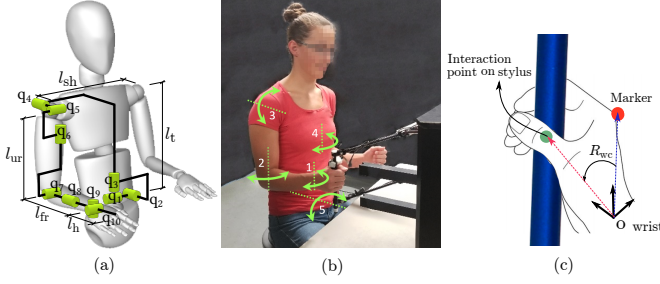


**Fig. 2:** (a) Kinematics model of human upper body, (b) Five motion routines for CPA segment length estimation, (c) Hand pose correction for MoCap in grasping the stylus using a fixed rigid-body transformation  $R_{wc}$ .

where  $\mathbf{q}_{\min}$  and  $\mathbf{q}_{\max}$  are the joint limits. The high degree-of-freedom in human kinematics makes this problem a *redundant* problem with an infinite number of solutions. We seek the solution closest to the true posture of the teleoperator.

#### IV. APPROACH

In this section, we provide an approximate solution for partially observable posture estimation in teleoperation using a particle filter. We provide the kinematics model of the human upper body with only one moving arm. Next, we discuss adopting a particle filter for inference in our problem. Finally, we detail using CPA for segment length estimation.

##### A. Human kinematics model

We use a 10-DOF kinematics model (Fig. 2(a)) to analyze the upper body motion of a human sitting on a chair and operating the leader robot. We assume the hips are fixed to a stationary chair with a known pose w.r.t. the robot. The parameters of this model ( $\psi$ ) include the length of each segment in the upper body model. We compare 3 techniques for segment length estimation: (1) *Full measurement*: manually measuring the segment lengths from anatomical landmarks on subject bodies [29], [30], (2) *Height measurement*: measuring the height of the subject and selecting the segment lengths fitting to 50-percentile populations from the ANSUR II anthropometric model ([31]), (3) *CPA analysis* where each subject repeats 5 motion routines described in Sec. IV-C.

We define the human's *state variables* as  $\mathbf{q} = [q_i]_{i=1:10}$ ,  $\dot{\mathbf{q}} = [\dot{q}_i]_{i=1:10}$  where  $q_i$  represents the angle of joint  $i$  (shown in Fig. 2(a)). We assume that the user's hand stays attached to the leader robot's stylus, as such we can transfer the pose of the hand from the human's frame to the robot's frame.

We encode human motion limits in two ways. First, we use fixed limits on the joint angles based on the biomechanics literature [32], [33]. Our supplementary document details the exact joint ranges. If an angle estimate exceeds its limits, we project the estimate to the closest limit. Second, we use the learned, pose-dependant joint limit model from [15] to ensure the validity of the posture.

The estimated posture of the torso has a high effect on the estimated posture of the arm. Using the full range of motion for the torso would cause challenges in our posture estimation due to the four degrees of redundancy in the kinematics model. To overcome this issue, other researchers

assumed that the torso posture is fully known and they only consider the arm [6]. Instead, we include the torso in the posture estimation problem by assuming that the torso stays close to the vertical position with a low variance. We incorporate this as a perturbation of the torso posture in the problem. This assumption is reasonable and was confirmed in our workstation where the teleoperator sits behind a table interacting with a haptic interface.

From the kinematics of human motion, we find joint angles and velocities based on the previous step as follows:

$$\dot{\mathbf{q}}_k = \dot{\mathbf{q}}_{k-1} + \ddot{\mathbf{q}}_{k-1}dt \quad (3)$$

$$\mathbf{q}_k = \mathbf{q}_{k-1} + \dot{\mathbf{q}}_k dt \quad (4)$$

We model joint accelerations generated from a Gaussian distribution  $\ddot{\mathbf{q}}_{k-1} \sim \mathcal{N}(0, \tilde{\Sigma}_v)$ . Since  $dt$  is fixed, setting  $\Sigma_v = \tilde{\Sigma}_v \cdot dt$  transforms Eq. (3) to:

$$p(\dot{\mathbf{q}}_k | \dot{\mathbf{q}}_{k-1}) \sim \mathcal{N}(\dot{\mathbf{q}}_{k-1}, \Sigma_v) \quad (5)$$

We model the observation likelihood function by a Gaussian distribution over the hand's pose and velocity as the end-effector of the human kinematic chain:

$$p([\mathbf{z}_k, \dot{\mathbf{z}}_k] | [\mathbf{q}_k, \dot{\mathbf{q}}_k]) = \mathcal{N}(\phi(\mathbf{q}_k, \dot{\mathbf{q}}_k, \psi), \Sigma_K) \quad (6)$$

in which  $\Sigma_K$  is the kinematic covariance matrix.

##### B. Particle Filter for Posture Estimation

We approximate the solution for the partially observable problem of posture estimation by using a particle filter [34] with some modifications. As the estimation of the 10-DOF human model from the trajectory of the leader robot has high ambiguity due to the redundancy, we add the joint angular velocities to our state variables and use the velocity of the leader robot's stylus in our observations. As a prior, we encode that the human *starts* the task in a static, neutral posture as shown in Fig. 2(b). We initialize  $M$  particles using a truncated normal distribution with the mean at the neutral posture  $\mathbf{q}_{neutral}$  and set the initial angular velocities to zero:

$$\mathbf{q}_0^{[m]} \sim \mathcal{N}(\mathbf{q}_{neutral}, \Sigma_0), \quad \dot{\mathbf{q}}_0^{[m]} = 0 \quad m = 1, \dots, M \quad (7)$$

where  $\Sigma_0 = 0.2 \times (\mathbf{q}_{\max} - \mathbf{q}_{\min})$  for each joint.

Each particle is propagated in time based on the kinematics of human motion using Eqs. 3 and 4. Then, the particles are weighted based on the observation likelihood function in Eq. (6) defined as the innovation error between the estimated pose of the stylus and the observed pose from the leader robot. We use the multivariate Gaussian distribution to define the likelihood weighting function:

$$w_k^{[m]} = v_p \cdot \det(2\pi\Sigma_K)^{-\frac{1}{2}} \cdot \exp\left\{-\frac{1}{2}([\mathbf{z}_k, \dot{\mathbf{z}}_k] - \phi(\mathbf{q}_k, \dot{\mathbf{q}}_k, \psi))^T \Sigma_K^{-1} ([\mathbf{z}_k, \dot{\mathbf{z}}_k] - \phi(\mathbf{q}_k, \dot{\mathbf{q}}_k, \psi))\right\} \quad (8)$$

where  $v_p \in \mathbb{R}, 0 \leq v_p \leq 1$ , encodes the validity of the posture as output of the learned neural network from [15].

### C. Circle Point Analysis for Segment Length Estimation

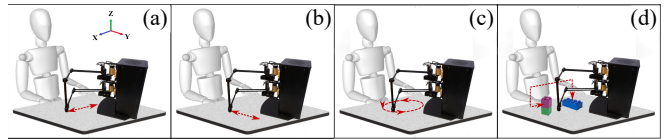
We estimate the segment lengths  $\psi$  through a calibration procedure variant of circle point analysis (CPA) [14]. Starting from the neutral posture, the user performs five predefined motion patterns that only include motion in one of their joints. When following such a pattern, we assume that the human hand will move on a circle. Estimating the circle parameters defines the location of the active joint and its distance from the end-effector. From this we derive the lengths of each arm segment.

Fig. 2(b) presents the 5 motion patterns used in data generation for CPA: (1) wrist flexion/extension to estimate hand length; (2) upper arm external/internal rotation to estimate forearm length; (3) upper arm abduction/adduction to estimate upper arm length; (4) rotation from the hip to estimate shoulder length; and (5) lateral bending from the hip to estimate torso length. We note that in estimating the last two segments we use the previously estimated arm and hand segment lengths.

### V. IMPLEMENTATION & EXPERIMENTAL PROTOCOL

We conducted a human subject experiment in which subjects interact with a 6-DOF Quanser HD<sup>2</sup> haptic interface as the leader robot (see Fig. 1). We recorded human motion using a 12-camera Optitrack [35] MoCap system for comparison. We collected data from 8 human subjects including 4 female and 4 male subjects with ages ranging from 25 to 33 years and heights in the range of  $171 \pm 21$ cm. Each subject performed 4 tasks visualized in Fig. 3: (1) following a straight line in the  $X$ -direction, (2) following a straight line in the  $Y$ -direction, (3) following a circular path, and (4) pick and place with an unprescribed motion and high range of wrist rotation. We provided a printed visual guide on the table for the first three tasks. The goal was to provide different types of motion for analysis; the subjects were not required to follow the path accurately. The robot collected data from the subject motion without exerting any force.

The gold-standard MoCap system estimates the upper-body posture for a 10-DOF torso, however, our human model only includes 3-DOF for the torso. To address this discrepancy, the MoCap posture is retargeted to our human model using the inverse kinematics. Moreover, the segment lengths are variable during a motion in MoCap data, while our model uses fixed lengths. This change is more visible in the forearm and upper arm, where we observed almost 2.3cm and 1.8cm of change, respectively, for a subject doing the circular task. This is mainly because the marker placement on the body will never be perfect, and motion is subject to some skin artifacts leading to this type of error [36]. Additionally, as shown in Fig. 2(c), the MoCap pose for the hand uses the segment from the wrist axis to the marker at the metacarpophalangeal joint of the index finger, while our human model uses the segment from the wrist joint to the interaction point. To correct for this, we use a fixed rigid-body transformation  $R_{wc}$  for the MoCap wrist joint calculated for each subject.



**Fig. 3:** Tasks for human subject experiments following (a) a straight line in the  $X$  direction, (b) a straight line in the  $Y$  direction, (c) a circular path, and (d) a pick and place with no target motion.

To compare with other well-known approaches, we solved the least-squares problem in Eq. (2) using two other deterministic methods: (1) boosted and bounded online least-squares IK optimization (*Online-IK*) in which we simply solve the inverse kinematics optimization independently at each time step by initializing it with the solution from the previous time step, and (2) boosted and bounded offline least-squares trajectory IK optimization (*Offline-TrajIK*) in which we solve the inverse kinematics problem for the whole trajectory by initializing it with the solution trajectory from the *Online-IK*. We used dogleg algorithm with rectangular trust regions from SciPy [37] as the optimization solver.

As neither marker-based nor markerless posture estimation techniques provide ground truth posture, we additionally provide qualitative analysis by overlaying the estimated posture on synchronized video frames. Fig. 9 shows the posture inferred by our approach aligns well with the MoCap estimates. We see some error due to our fixed segment lengths assumption for MoCap motion. While other possible approaches of analysis exist (e.g. hand-labeling points [38]), these approaches are error prone and time-consuming.

In our implementation, we use a fixed number of particles ( $M=500$ ), as this appears to work well across a large number of tasks in the experimental trials. Deriving the kinematic covariance matrix is included in the supplementary document.

For the risk assessment on both the estimated postures from our approach and the MoCap estimates, we use the following assumptions for all tasks: the human is sitting on a chair, minimal intermittent force/load ( $<2.0$ Kg), muscle use occurrence less than 4x per minute, untwisted and vertical position for neck and torso, and supported legs and feet.

### VI. RESULTS & DISCUSSION

This section provides results from our human subject experiments. We discuss the performance of the proposed approach comparing with MoCap, as well as the estimated risk assessment results. We compare the deviation<sup>2</sup> of estimated segment lengths from MoCap lengths using the various methods discussed in Section IV-A, among all subjects in Fig. 4. The deviation for *full-measurement* lengths of the hand is zero since the MoCap marker set did not provide a representative length for the hand. We used the *full measurement* value instead. The last three columns of the figure (All) shows the deviation for all of the segments. Statistical analyses reveal that *CPA* lengths deviate least from the MoCap lengths significantly<sup>3</sup>. The main reason that *CPA*

<sup>2</sup>We use the term “deviation” instead of “error” since the MoCap posture is also an estimate and not ground truth.

<sup>3</sup>We use  $\alpha = 0.05$  for statistical analysis.



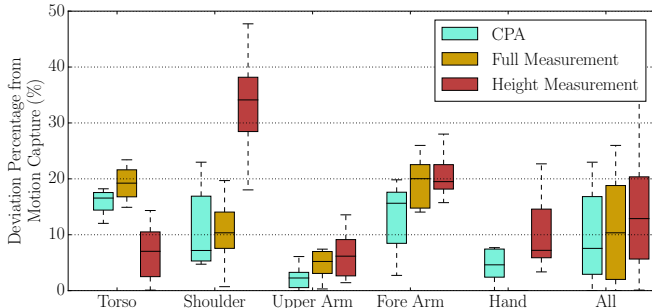


**Fig. 4:** Deviation of segments lengths from the MoCap lengths.

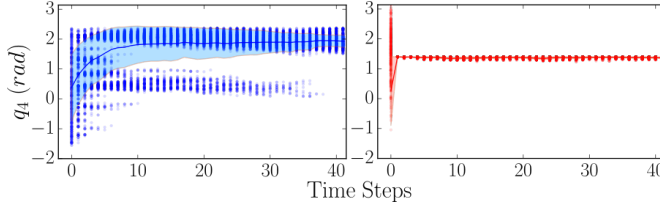


**Fig. 5:** Behaviour of particles through time for the shoulder abduction joint of subject 1 during the circular task. (left) Particles initialized uniformly over the ROM with higher diagonal values of  $\Sigma_K$ . (right) Particles initialized from a normal distribution with the mean at the neutral posture and lower diagonal values of  $\Sigma_K$ .

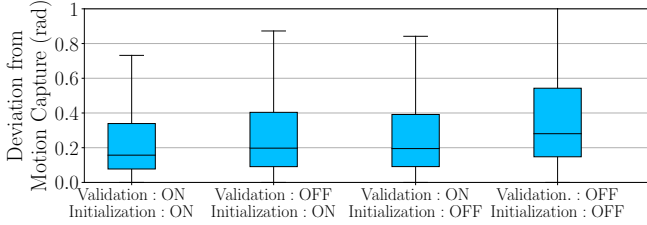
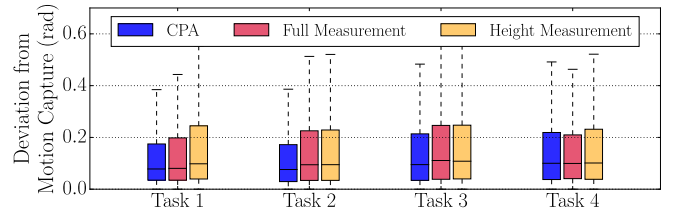


**Fig. 6:** The effect of initialization and posture validation on posture estimation in trials of the circular and the horizontal tasks.

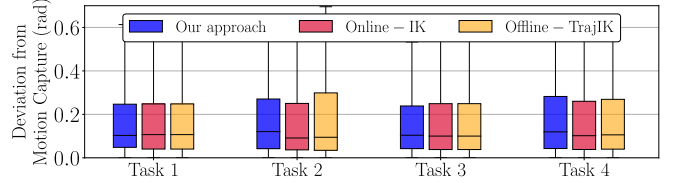
deviates less than *full measurement* is that the anatomical landmarks used for manual measurement of the segments lengths are not necessarily on the joint axes calculated by the MoCap from the markers. Actual length values are included in the supplementary document.

Fig. 5 shows the evolution of all the particles in a circular task as well as the mean and standard deviation of their distributions. On the left, we initialize particles from a uniform distribution over a joint's ROM and use high values of kinematic covariance (0.1 for position, 0.5 for orientation). In this case, particles from multiple modes are kept for about 40 steps, then they converge into a single mode. On the right, we initialize particles from a normal distribution around the neutral posture and use the kinematic covariance matrix  $\Sigma_K$  as described in the supplementary document. The particles converge quickly to the correct mode. This shows the effect of initializing the particles around the neutral posture.

Moreover, Fig. 6 shows the comparison between the effect of initialization around the neutral posture and validation of the posture based on the pose-dependant ROM for 4 trials of the horizontal and 4 trials of the circular tasks. We can see that the combination of these two methods reduces the deviation, however, the effect of each one is almost equal.



**Fig. 7:** Deviation of the posture estimated by the proposed approach from MoCap system for all the subjects in different tasks.



**Fig. 8:** Deviation of the posture estimated by our approach vs Online-IK and Offline-TrajIK methods among all the tasks.

This implies that in some applications, it is safe to just use the initialization around the neutral posture instead of the computationally-expensive validation of each particle.

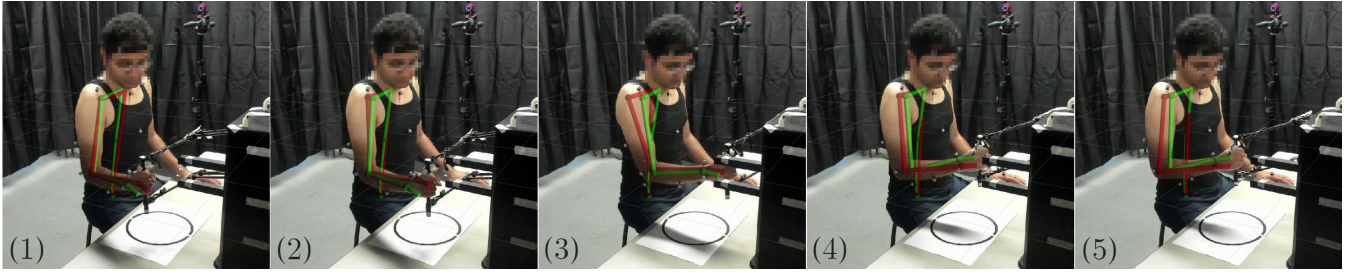
Fig. 7 represents the deviation between the posture from our approach and the posture from MoCap for all the subjects, and trials across the tasks using different segment length estimation methods. Overall, the approach generally agrees with a median deviation less than 0.09rad (less than 5deg) and upper quartile less than 0.25rad (less than 15deg) considering the observation solely from the stylus trajectory and having no extra sensors. Statistical analysis for comparing the effect of all three segment length estimation methods on the posture estimation accuracy reveals that *CPA* method has a significantly lower deviation from the MoCap posture where there is no significant difference between the *full-measurement* and *height-measurement* methods.

Fig. 8 compares our posture estimation approach with two other least-squares IK solutions of redundant robots for all subjects, among 4 tasks using *CPA* lengths. From the statistical analysis of the results, we can conclude that our probabilistic *particle filter* approach performance is not significantly different than the other two methods.

Fig. 9 illustrates video frames of a subject during the circular task with overlaid reconstructed skeletons from MoCap (green) and our approach (red) as a qualitative evaluation. The estimated posture aligns well with the observed posture during the entire task. Although the leader robot's trajectory is smooth, the video shows non-smooth estimations from our approach, which is due to the characteristics of the particle filter and plotting the most-probable posture.

We plot the expected value of the RULA score and its standard deviation over time using the posture estimates from our particle filter in Fig. 10. As mentioned earlier, unlike the deterministic estimators, our probabilistic approach provides an estimated distribution over posture and hence, a distribution over estimated RULA scores. Higher expected RULA scores correspond to postures where the subject gets closer to the end of horizontal motion.

Fig. 11 shows the maximum RULA score in a task (the



**Fig. 9:** Video-overlaid skeletons show the posture (most probable particle) estimated from our proposed approach (red) and MoCap (green).

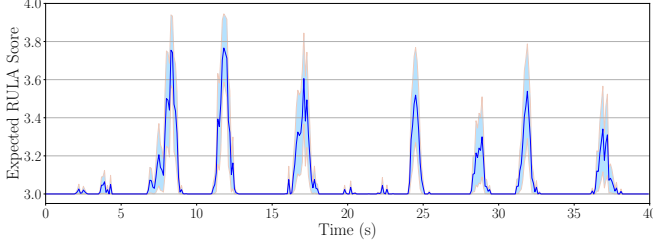


**Fig. 10:** Expected RULA score (solid line) and standard deviation (shaded region) over time for subject 1 performing task 1.

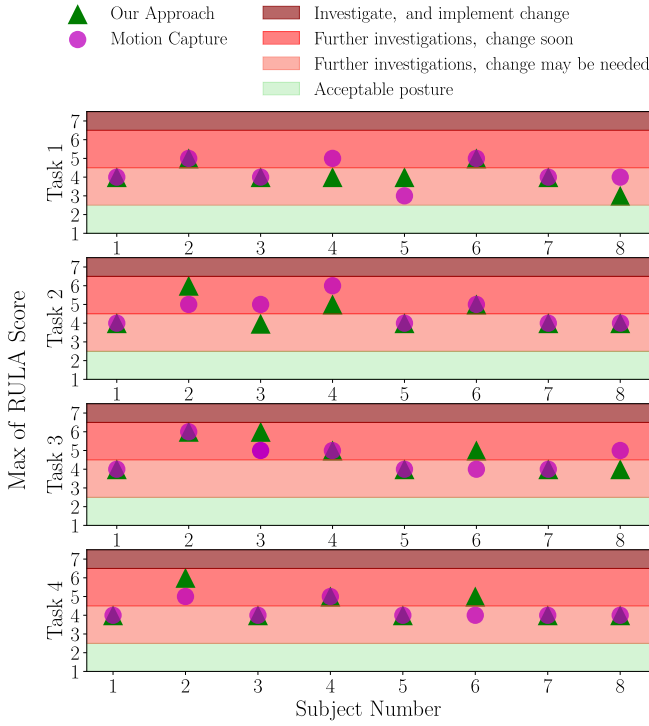


**Fig. 11:** Comparison of the maximum value of RULA scores of a task using estimated posture from our approach and MoCap for all the subjects and trials.

one most often used in ergonomics) for both our approach and the MoCap posture estimates. Our proposed approach was successful in identifying all instances where the RULA score was higher than 2 in all 32 trials. The experiment resulted in the same interpretation of the RULA score in 27 trials (84.37%) and the same RULA score in 21 trials (65.63%). Our approach estimates the same RULA score (not the maximum value for task) across all trajectories and subjects with median accuracy of more than 86.4% for task 1 and 2, and more than 74.7% for task 3 and 4.

Overall, the results show that the proposed posture estimation solely from the leader robot has the potential to be used for continuous monitoring of ergonomics during teleoperation. Our approach is also accurate enough to provide alerts when further ergonomics investigation is required.

## VII. CONCLUSION

In this paper, we investigated if a leader robot is an adequate sensor to continuously monitor posture to assess the ergonomics of a human-teleoperated task. We described a probabilistic approach which is based solely on the data recorded from a leader robot's end-effector, that is already necessary to perform the teleoperation task. We compared our approach with well-known *Online-IK* and *Offline-TrajIK* methods for human inverse kinematics. We used CPA to estimate segment lengths and utilized RULA for risk assessment.

Our results show that the leader robot is an adequate sensor for human posture estimation and ergonomic assessment in applications such as continuous monitoring of the human teleoperator. More specifically, we found that CPA estimates more accurate segment lengths and the proposed algorithm can successfully estimate the posture based solely on the leader robot's stylus trajectory with a low deviation from MoCap. We also showed that our approach agrees with MoCap postures similar to *Online-IK* and *Offline-TrajIK*, providing a probabilistic distribution for the posture. Furthermore, the risk assessment results show that our proposed approach resulted in the same interpretation of the RULA score in 27 of 32 trials (84.37%), and the same maximum RULA score in 21 trials (65.63%). This is sufficient to trigger further assessment to investigate ergonomic hazards.

In this paper, we focused on teleoperation applications, which has a high prevalence of WMSDs. However, it is possible to extend it to other physical human-robot interaction tasks such as programming by demonstration and co-manipulation. We assumed a seated teleoperator in this paper, but we can extend our approach to a standing teleoperator by adding the foot pose as a state variable. It would be straightforward to combine our proposed approach with other sensing modalities (e.g., vision or MoCap) when available in a specific application context by integrating these additional observations into the particle filter weighting scheme.

Future work will focus on increasing the complexity of the human model (e.g. adding muscle activation). Additionally, we are examining substituting the particle filter with an incremental smoothing method [39] in order to improve estimation results and decrease runtime.

## REFERENCES

- [1] A. M. Zanchettin, N. M. Ceriani, P. Rocco, H. Ding, and B. Matthias, "Safety in human-robot collaborative manufacturing environments: Metrics and control," *IEEE Transactions on Automation Science and Engineering*, vol. 13, no. 2, pp. 882–893, 2016.
- [2] D. Fridovich-Keil, A. Bajcsy, J. F. Fisac, S. L. Herbert, S. Wang, A. D. Dragan, and C. J. Tomlin, "Confidence-aware motion prediction for real-time collision avoidance," *The International Journal of Robotics Research*, vol. 39, no. 2-3, pp. 250–265, 2020.
- [3] K. Mangalam, E. Adeli, K.-H. Lee, A. Gaidon, and J. C. Niebles, "Disentangling human dynamics for pedestrian locomotion forecasting with noisy supervision," in *The IEEE Winter Conference on Applications of Computer Vision*, 2020, pp. 2784–2793.
- [4] A. Casalino, D. Bazzi, A. M. Zanchettin, and P. Rocco, "Optimal proactive path planning for collaborative robots in industrial contexts," in *2019 International Conference on Robotics and Automation (ICRA)*. IEEE, 2019, pp. 6540–6546.
- [5] J. Mainprice, E. A. Sisbot, T. Siméon, and R. Alami, "Planning safe and legible hand-over motions for human-robot interaction," in *IARP/IEEE-RAS/EURON workshop on technical challenges for dependable robots in human environments*, 2010.
- [6] R. Rahal, G. Matarese, M. Gabiccini, A. Artoni, D. Prattichizzo, P. R. Giordano, and C. Pacchierotti, "Caring about the human operator: haptic shared control for enhanced user comfort in robotic telemanipulation," *IEEE Transactions on Haptics*, vol. 13, no. 1, pp. 197–203, 2020.
- [7] T. Vos, R. M. Barber, B. Bell, A. Bertozzi-Villa, S. Biryukov, I. Bolliger, F. Charlson, A. Davis, L. Degenhardt, D. Dicker, et al., "Global, regional, and national incidence, prevalence, and years lived with disability for 301 acute and chronic diseases and injuries in 188 countries, 1990–2013: a systematic analysis for the Global Burden of Disease Study 2013," *The Lancet*, vol. 386, no. 9995, pp. 743–800, 2015.
- [8] P. G. Dempsey, L. M. Kocher, M. F. Nasarwanji, J. P. Pollard, and A. E. Whitson, "Emerging ergonomics issues and opportunities in mining," *International journal of environmental research and public health*, vol. 15, no. 11, p. 2449, 2018.
- [9] M. Alvarez, D. Torricelli, A. J. del Ama, D. Pinto, J. Gonzalez-Vargas, J. C. Moreno, A. Gil-Agudo, and J. L. Pons, "Simultaneous estimation of human and exoskeleton motion: a simplified protocol," in *IEEE Int. Conf. on Rehabilitation Robotics*, 2017, pp. 1431–1436.
- [10] X. Xiao and S. Zarar, "A wearable system for articulated human pose tracking under uncertainty of sensor placement," in *IEEE Int. Conf. on Biomedical Robotics and Biomechatronics*, 2018, pp. 1144–1150.
- [11] X. Chen and J. Davis, "Camera placement considering occlusion for robust motion capture," Computer Graphics Laboratory, Stanford University, Tech. Rep., Tech. Rep., 2000.
- [12] A. Erol, G. Bebis, M. Nicolescu, R. D. Boyle, and X. Twombly, "Vision-based hand pose estimation: A review," *Computer Vision and Image Understanding*, vol. 108, no. 1-2, pp. 52–73, 2007.
- [13] B. Busch, G. Maeda, Y. Mollard, M. Demangeat, and M. Lopes, "Postural optimization for an ergonomic human-robot interaction," in *2017 IEEE/RSJ International Conference on Intelligent Robots and Systems (IROS)*. IEEE, 2017, pp. 2778–2785.
- [14] B. W. Mooring, Z. S. Roth, and M. R. Driels, *Fundamentals of manipulator calibration*. Wiley New York, 1991.
- [15] Y. Jiang and C. K. Liu, "Data-driven approach to simulating realistic human joint constraints," in *2018 IEEE International Conference on Robotics and Automation (ICRA)*. IEEE, 2018, pp. 1098–1103.
- [16] L. McAtamney and E. N. Corlett, "RULA: a survey method for the investigation of work-related upper limb disorders," *Applied ergonomics*, vol. 24, no. 2, pp. 91–99, 1993.
- [17] P. Vartholomeos, N. Katevas, A. Papadakis, and L. Sarakis, "Design of motion-tracking device for intuitive and safe human-robot physical interaction," in *IEEE Int. Conf. on Telecommunications and Multimedia*, 2016, pp. 1–6.
- [18] J. Buzzi, E. De Momi, and I. Nisky, "An uncontrolled manifold analysis of arm joint variability in virtual planar position and orientation tele-manipulation," *IEEE Transactions on Biomedical Engineering*, 2018.
- [19] G. Martinez, I. A. Kakadiaris, D. Magruder, and I. Magruder, "Tele-operating ROBONAUT: A case study," in *British Machine Vision Conference*, 2002, pp. 1–10.
- [20] R. J. Mozhdzhehi, Y. Reznichenko, A. Siddique, and H. Medeiros, "Deep convolutional particle filter with adaptive correlation maps for visual tracking," in *IEEE Int. Conf. on Image Processing*, 2018, pp. 798–802.
- [21] T. Zhang, S. Liu, C. Xu, B. Liu, and M. Yang, "Correlation particle filter for visual tracking," *IEEE Transactions on Image Processing*, vol. 27, no. 6, pp. 2676–2687, 2018.
- [22] R. Van Der Merwe, A. Doucet, N. De Freitas, and E. A. Wan, "The Unscented Particle Filter," in *Advances in neural information processing systems*, 2001, pp. 584–590.
- [23] R. Poppe, "Vision-based human motion analysis: An overview," *Computer vision and image understanding*, vol. 108, no. 1-2, pp. 4–18, 2007.
- [24] X. Wang, M. Maurin, F. Mazet, N. D. C. Maia, K. Voinot, J. P. Verriest, and M. Fayet, "Three-dimensional modelling of the motion range of axial rotation of the upper arm," *Journal of biomechanics*, vol. 31, no. 10, pp. 899–908, 1998.
- [25] I. Akhter and M. J. Black, "Pose-conditioned joint angle limits for 3D human pose reconstruction," in *Proceedings of the IEEE conference on computer vision and pattern recognition*, 2015, pp. 1446–1455.
- [26] S. A. Ismail, S. B. M. Tamrin, M. R. Baharudin, M. A. M. Noor, M. H. Juni, J. Jalaludin, and Z. Hashim, "Evaluation of two ergonomics intervention programs in reducing ergonomic risk factors of musculoskeletal disorder among school children," *Res J Med Sci*, vol. 4, no. 1, pp. 1–10, 2010.
- [27] Z. Khodabakhshi, S. A. Saadatmand, M. Anbarian, and R. Heydari Moghadam, "An ergonomic assessment of musculoskeletal disorders risk among the computer users by rula technique and effects of an eight-week corrective exercises program on reduction of musculoskeletal pain," *Iranian Journal of Ergonomics*, vol. 2, no. 3, pp. 44–56, 2014.
- [28] S. Hignett and L. McAtamney, "Rapid entire body assessment (REBA)," *Applied ergonomics*, vol. 31, no. 2, pp. 201–205, 2000.
- [29] S. Pheasant and C. M. Haslegrave, *Bodyspace: Anthropometry, ergonomics and the design of work*. CRC press, 2018.
- [30] W. T. Dempster, "Space requirements of the seated operator, geometrical, kinematic, and mechanical aspects of the body with special reference to the limbs," Michigan State Univ East Lansing, Tech. Rep., 1955.
- [31] R. C. Fromuth and M. B. Parkinson, "Predicting 5th and 95th percentile anthropometric segment lengths from population stature," in *ASME International Design Engineering Technical Conferences and Computers and Information in Engineering*, 2009, pp. 581–588.
- [32] P. K. Levangie and C. C. Norkin, "Joint structure and function; a comprehensive analysis. 3rd," Philadelphia: FA. Davis Company, 2000.
- [33] "NASA man-system integration standard," Available at <https://msis.jsc.nasa.gov/sections/section03.htm> (09/16/2020).
- [34] S. Thrun, W. Burgard, and D. Fox, *Probabilistic robotics*. MIT press, 2005.
- [35] "NaturalPoint Inc., Corvallis, OR," <https://optitrack.com/> (09/16/2020).
- [36] C. Metcalf, C. Phillips, A. Forrester, J. Glodowski, K. Simpson, C. Everitt, A. Darekar, L. King, D. Warwick, and A. Dickinson, "Quantifying Soft Tissue Artefacts and Imaging Variability in Motion Capture of the Fingers," *Annals of Biomedical Engineering*, pp. 1–11, 2020.
- [37] P. Virtanen, R. Gommers, T. E. Oliphant, M. Haberland, T. Reddy, D. Cournapeau, E. Burovski, P. Peterson, W. Weckesser, J. Bright, et al., "SciPy 1.0: fundamental algorithms for scientific computing in Python," *Nature methods*, vol. 17, no. 3, pp. 261–272, 2020.
- [38] V. Athitsos and S. Sclaroff, "Estimating 3D hand pose from a cluttered image," in *IEEE Conference on Computer Vision and Pattern Recognition*, vol. 2, 2003, pp. II–432.
- [39] M. Kaess, H. Johannsson, R. Roberts, V. Ila, J. J. Leonard, and F. Dellaert, "iSAM2: Incremental smoothing and mapping using the Bayes tree," *The International Journal of Robotics Research*, vol. 31, no. 2, pp. 216–235, 2012.

# Is The Leader Robot an Adequate Sensor for Posture Estimation and Ergonomic Assessment of A Human Teleoperator? (Supplementary Document)

Amir Yazdani\*, Roya Sabbagh Novin\*, Andrew Merryweather\*, and Tucker Hermans†

## I. HUMAN KINEMATICS

We use human biomechanics ([?], [?]) to define the fixed range of motion constraints in the posture estimation problem. Based on the type of the teleoperation tasks, we assume that the torso stays around the vertical position with a low variance. Table I shows the joint limits we used with the reference to the T-pose as the zero-angle configuration.

## II. PARTICLE FILTER FOR POSTURE ESTIMATION

In this paper, we follow the particle filter algorithm presented in [?]. For the kinematic covariance matrix, we use a diagonal covariance matrix as:

$$\Sigma_K = 0.01 \cdot \text{diag}(0.001, 0.001, 0.001, 0.05, 0.05, 0.05, 1.0, 1.0, 1.0, 10, 10, 10), \quad (1)$$

and define the acceleration covariance as:

$$\Sigma_v = 0.01 \cdot \text{diag}(0.01, 0.01, 0.01, 0.05, 0.05, 0.05). \quad (2)$$

These parameters have been tuned based on one subject and used for all subjects without any modification.

## III. SEGMENT LENGTH ESTIMATION

Estimated and measured segment lengths for all the subjects are provided in Table II. We compare the deviation of estimated segment lengths from the different methods from the manually measured lengths among all subjects in Fig. 1. The deviation for lengths of hand estimated by motion capture from the fully-measured lengths is zero because the mocap could not provide a length for the hand, so we used the manually measured one instead of it. The last column of the figure shows that lengths from CPA deviate less from the measured lengths.

## IV. RESULTS & DISCUSSION

Figure 2 shows the deviation between the posture from our approach and the posture from MoCap for all the subjects, tasks, and trials across the joints using three different segment length estimation methods. Overall, the approaches generally agree and in the worst case, we see a median deviation less than 0.18rad (less than 11deg) and upper quartile less than 0.32rad (less than 18deg) for  $q_9$ , considering the observation solely from stylus trajectory and having no extra sensors.

Joint Name	Description	Min (deg)	Max (deg)
$q_1$	Torso flexion	-5	15
$q_2$	Torso lateral bending	-5	5
$q_3$	Torso rotation	-10	10
$q_4$	Shoulder abduction	-90	135
$q_5$	Shoulder vertical flexion	-90	90
$q_6$	Shoulder horizontal flexion	-45	135
$q_7$	Elbow flexion	0	150
$q_8$	Elbow supination	-70	70
$q_9$	Hand radial deviation	-30	20
$q_{10}$	Hand flexion	-45	45

**TABLE I:** Range of motion for the joints in the human kinematics model

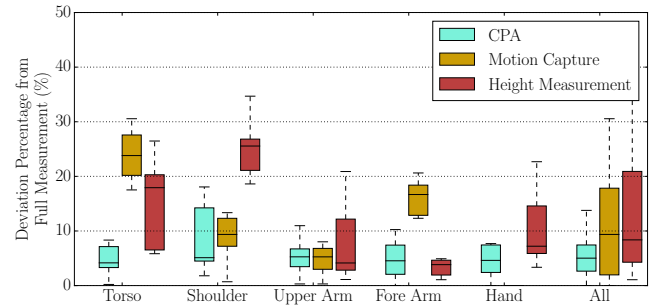


**Fig. 1:** Deviation of segments lengths from the measured lengths.

We see that the deviation is very low for torso orientation ( $q_1, q_2, q_3$ ) since they are limited to a low range of motion. The deviations increase in the shoulder joints ( $q_4, q_5, q_6$ ) and we see higher deviations in the elbow joint ( $q_7$ ). This deviation is mainly due to the deviation in forearm and upper arm lengths which cause the particle filter to increase or decrease the elbow flexion angle to keep the hand attached to the stylus. We also see deviation in wrist joints ( $q_8, q_9, q_{10}$ ) which can be caused by the error in the fixed rigid-body transformation that we used to correct the hand pose in the MoCap data.

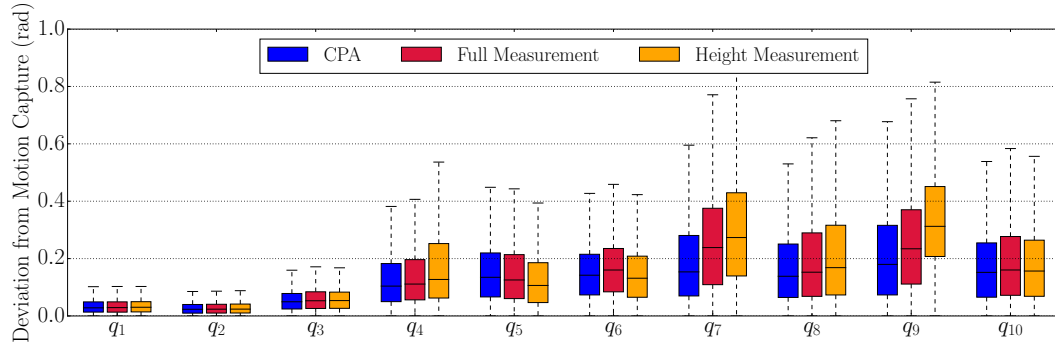
\*Department of Mechanical. Eng. and Robotics Center, University of Utah, Salt Lake City, UT, USA, amir.yazdani@utah.edu

†School of Computing and Robotics Center, University of Utah, Salt Lake City, UT, USA



**TABLE II:** Subject information in the human subject experiment.

Segments/Data	Estimation Type	Subject Number							
		1	2	3	4	5	6	7	8
Age (year)	-	29	30	32	26	29	25	31	33
Height (mm)	Full-Measure	1720	1680	1500	1920	1530	1570	1690	1690
Torso (mm)	CPA	475	479	395	497	396	390	424	478
	Full-Measure	476	412	411	480	371	360	406	466
	Height-Measure	505	487	435	564	443	455	496	496
	Mocap	576	530	483	565	472	470	500	580
Shoulder (mm)	CPA	368	380	366	394	298	310	340	401
	Full-Measure	352	334	310	416	284	324	334	346
	Height-Measure	442	420	375	493	382	392	434	434
	Mocap	305	309	386	374	282	296	294	368
Upper Arm (mm)	CPA	331	308	263	308	284	273	297	304
	Full-Measure	330	293	237	310	304	294	314	318
	Height-Measure	333	320	286	372	292	299	327	327
	Mocap	329	315	256	328	284	287	304	303
Forearm (mm)	CPA	256	241	216	272	221	210	217	226
	Full-Measure	259	257	211	280	221	234	232	269
	Height-Measure	263	245	219	293	223	229	258	258
	Mocap	218	204	185	227	193	193	202	220
Hand (mm)	CPA	66	69	70	77	62	73	94	68
	Full-Measure	66	67	65	75	61	68	80	64
	Height-Measure	62	62	55	70	56	58	61	61
	Mocap	66	67	65	75	61	68	80	64

**Fig. 2:** Deviation of the posture estimated by the proposed approach from MoCap system for all the trials.